doi:10.1016/j.jmb.2007.06.057 J. Mol. Biol. (2007) 372, 535–548

JMB

Available online at www.sciencedirect.com

ScienceDirect

ELSEVIER

CTL Recognition of a Protective Immunodominant Influenza A Virus Nucleoprotein Epitope Utilizes a Highly Restricted Vβ but Diverse Vα Repertoire: Functional and Structural Implications

Weimin Zhong[1]*, Surjit B. Dixit[2], Robert J. Mallis[3], Haribabu Arthanari[3] Alexey A. Lugovskoy[4], David L. Beveridge[2], Gerhard Wagner[3] and Ellis L. Reinherz[1]*

[1]*Laboratory of Immunobiology and Department of Medical Oncology, Dana-Farber Cancer Institute, 77 Avenue Louis Pasteur, Boston, MA 02115 USA*

[2]*Department of Chemistry and Molecular Biophysics Program Hall-Atwater Laboratories Wesleyan University Middletown, CT 06459, USA*

[3]*Department of Biological Chemistry and Molecular Pharmacology, Harvard Medical School, 240 Longwood Avenue Boston, MA 02115, USA*

[4]*Molecular Modeling, Biogen Idec Inc., 14 Cambridge Center Cambridge, MA 02142, USA*

**Corresponding authors*

To investigate protective immunity conferred by CTL against viral pathogens, we have analyzed $CD8^+$ T cell responses to the immunodominant nucleoprotein epitope ($NP_{366–374}$) of influenza A virus in B6 mice during primary and secondary infections *in vivo*. Unlike the highly biased TCR Vβ repertoire, the associated Vα repertoire specific for the $NP_{366–374}/D^b$ ligand is quite diverse. Nonetheless, certain public and conserved CDR3α clonotypes with distinct molecular signatures were identified. Pairing of public Vα and Vβ domains creates an αβ TCR heterodimer that binds efficiently to the $NP_{366–374}/D^b$ ligand and stimulates T cell activation. In contrast, private TCRs, each comprising a distinct α chain paired with the same public β chain, interact very differently. Molecular dynamics simulation reveals that the conformation and mobility of the shared Vβ CDR loops are governed largely by the associated Vα domains. These results provide insight into molecular principles regarding public *versus* private TCRs linked to immune surveillance after infection with influenza A virus.

Keywords: influenza A virus; αβT cell receptors; immune recognition; molecular modeling; molecular dynamics

Introduction

$CD8^+$ cytotoxic T lymphocytes (CTL) play a key role in protecting the mammalian host against many viral infections.[1] This cellular immunity requires that $CD8^+$ T cells recognize virus-derived antigenic peptides bound to self-major histocompatibility complex molecules (pMHC) *via* clonally distributed T cell receptors (TCRs).[2] αβTCRs are membrane-bound heterodimers composed of α and β-subunits with structurally variable (V) amino-terminal domains.[3–5] Upon encounter with antigen, an array of TCRs is normally selected in response to the antigenic stimulus in the peripheral lymphoid system. This pool of receptors, termed the TCR repertoire, is comprised of αβTCRs

Present address: W. Zhong, Influenza Division, National Centers of Infectious Diseases, Centers for Disease Control and Prevention, Mailstop G-16, 1600 Clifton Road, Atlanta, GA 30333, USA.

Abbreviations used: CTL, cytotoxic T lymphocytes; pMHC, peptide bound to self-major histocompatibility complex molecules; TCR, T cell receptor; RACE, rapid amplification of cDNA ends; MFI, mean fluorescence intensity; PMA, phorbol 12-myristate 13-acetate.

E-mail addresses of the corresponding authors: wzhong@cdc.gov; ellis_reinherz@dfci.harvard.edu

0022-2836/$ - see front matter

differing from each other, yet having the ability to recognize the same pMHC ligand.

The diversity, clonality and specificity of an antigen-specific TCR repertoire depend on the molecular, biophysical and structural natures of both Vα and Vβ domains comprising each αβ heterodimer. A large body of literature has been generated in attempting to correlate TCR usage with the recognition of a specific viral or tumor pMHC ligand.[6] Evidence accumulated so far indicates that TCR repertoires selected in response to a given pMHC ligand appear either rather diverse or highly restricted, depending on the experimental systems under investigation. However, to date, this assessment of antigen-selected TCR repertoire diversity has been reliant on either analyses of a limited number of *in vitro* CTL clones or *ex vivo* molecular tracking of antigen-specific TCR Vβ chain repertoires. The contribution of the associated Vα chains on clonal diversity and specificity of the TCR repertoires has been largely neglected because of technical complexity arising from the greater number of Vα and Jα germline segments. Moreover, there is little information on the biophysical, structural and functional natures of the characterized TCR repertoires, which may profoundly impact the antiviral capability of the CTLs expressing these TCRs.

Recently, we have conducted an *ex vivo* analysis of the TCR β chain repertoire in response to an H-2D^b-restricted, immunodominant $NP_{366–374}$ (NP_{366}) CTL epitope of influenza A virus[7] that has been shown to induce strong protective cellular immunity against viral challenge in B6 mice.[8] It was found, unexpectedly, that the viral NP_{366}/D^b ligand-selected immune TCR β chain repertoire is highly biased, characterized by prominent usage of the TRBV13-1-TRBD1-TRBJ2-2 gene segment combination and a strong selection of CDR3β clonotypes with a nine amino acid residue segment. Detailed analysis of the molecular features of the CDR3β clonotypes reveal that, although a considerable proportion of the distinct, e.g. "private", CDR3β clonotypes exists during the primary response, clonal compositions of the CDR3β loops become highly focused after a second exposure to the influenza A virus. In fact, the majority of the CDR3β loops identified within the secondary immune TCR Vβ repertoire possess identical amino acid sequences with only three residue variations documented at a given position of these CDR3β loops. Most importantly, one CDR3β clonotype with the GxN sequence motif is selected by all of the individual animals analyzed for recognition of the NP_{366}/D^b ligand of the influenza A virus. This "public" TCR β chain (referred to as the common TRB13-2 β chain) alone accounts for more than 40% of the CDR3β clonotypes within the secondary TCR Vβ repertoire analyzed in our study and was confirmed independently by Kedzierska and colleagues.[9]

Selection of antigen-specific "public" TCRs has been observed in a limited number of studies. For example, it has been documented that CTLs from unrelated HLA-B8$^+$ individuals use the same TCR α and β chain pairing for recognition of an immunodominant peptide derived from the latent antigen EBNA3A of Epstein-Barr virus. Remarkably, this shared TCR consists of the identical TCR Vα, Jα gene segment (TRAV26-2, TRAJ2-7) and αN-region as well as identical TCR Vβ, Dβ and Jβ (TRBV7-8, TRBD1/D2, TRBJ2-7) and βN-region sequences.[10] Another example involves influenza A virus infection in the HLA-A2$^+$ human population: the TCR β chain repertoire specific for the HLA-A2-restricted, immunodominant $M1_{58–66}$ ($M1_{58}$) CTL epitope of the virus is characterized by prominent usage of the TRBV17 family and the $^{I}/_{S}RS^{A}/_{S}$ amino acid motifs within the CDR3β regions.[11] Among these highly conserved TCR β chains selected, the CDR3β clonotype with the IRSS motif is particularly prominent and used by HLA-A2$^+$ individuals after infection with influenza A virus. On the other hand, several recent studies employing an *ex vivo* measure of the TCR β repertoires were unable to detect public TCRs to certain MHC class I-restricted viral CTL epitopes after infection with particular human viral pathogens, including herpes simplex virus and HIV.[12–14]

Together, the accumulating data suggest that selection of public and private TCRs appear to be associated with certain TCRs and/or pMHC ligands whose precise molecular and structural features are poorly understood. Limited analysis of Vα repertoires has contributed to this paucity of information. Here, we report that the TCR α chain repertoires specific for the immunodominant, protective NP_{366}/D^b ligand of influenza A virus have a profound impact on the clonal diversity, biophysical and immunological nature of the public and private TCRs selected by this pMHC ligand.

Results

Diverse TCR α chains are selected to pair with the highly-conserved TRB13-2 TCR β chain for recognition of the NP_{366}/D^b ligand

Earlier, we observed that the TCR β chain repertoire selected to recognize the immunodominant NP_{366}/D^b ligand of influenza A virus is remarkably biased and includes a public β chain (TRB13-2) comprised of TRBV13-1-TRBD1-TRBJ2-2 segments.[7] To understand the molecular features of the TCR α chains paired with this highly conserved TCR β chain repertoire, we conducted a comprehensive *ex vivo* molecular analysis of the associated TCR α chain repertoire.

CD8$^+$ NP_{366}/D^b tetramer$^+$ TRBV13-1$^+$ cells were first sorted from the spleens of individual mice after primary or secondary infection with the influenza A virus strains PR8 and x31, respectively, which share six of eight RNA genome segments including NP. The nucleotide sequences of the various elements of the rearranged TCR α chains, including the Vα, Jα gene segment and the hypervariable CDR3α junction regions, were then determined by 5′-rapid amplification of cDNA ends (RACE) PCR in combination with high-throughput DNA sequencing.

For clarity, the results are combined from three individual animals after primary or secondary infection, and only the Vα, Jα gene segment usage and the deduced amino acid sequences of the CDR3α regions are presented. Detailed information on the analysis of the individual animals is provided in Supplementary Data Table S3. As shown in Table 1, overall, a wide spectrum of Vα and Jα gene segments is selected to pair with the highly biased TRBV13-1 Vβ gene segment. A total of 45 out of 81 known murine Vα gene segment sequences, and 35 out of 58 known murine Jα gene segment sequences were detected from a total of 647 cDNA clones.

Table 1. Diverse TCR α chains are paired with the highly conserved TRBV13-1 TCR β chains to recognize the NP_{366}/D^b ligand derived from influenza A virus

Primary			Secondary		
Vα	CDR3α	Jα	Vα	CDR3α	Jα
7-3	SGSWQL	22	7-3	RNRI	31
6D-7	NAGAKL	39	11	EGYQNF	49
4D-3	GNMGYKL	9	16	RSNTRI	31
6D-3	GDMGYKL	9	6-5	GNQGKL	23
4D-3	RNSNNRI	31	12D-1	NNTGKL	17
8-1	ALNTGKL	27	5-4	NAGAKL	39
16	RGSGTYQ	13	5-4	RNSNNRI	31
16	RERAGNKL	17	4D-3	RNSNNRI	31
16	RANSGTYQ	13	4D-3	SNSGTYQ	13
16	RDSNYNVL	21	5-1	SGSNNRI	31
14-3	SRSNTNKV	34	9D-4	SAREAEL	15
16	RTSSGQKL	16	16	RTNSGTYQ	13
6-6	GGTGGYKV	12	16	RRNSGTYQ	13
16	RGNSGTYQ	13	6-3	RGAGGYKV	12
9-3	SATPIPTK	12	16	RTASLGKL	24
4D-3	FLDSNYQL	33	12-2	SSQGGRAL	15
5-1	PSNMGYKL	9	16	RGNSGTYQ	13
1	RDNSAGNKL	17	16	RANSGTYQ	13
16	REVQGGRAL	15	16	REVSGTYQ	13
16	REQQQRQQT	7	16	RNSSGTYQ	13
6-5	GASSGSWQL	22	12-1	GGSALGRL	18
6-6	GANTNTGKL	27	3-3	ATSSGQKL	16
14-3	SRTTNTGKL	27	6D-7	AYQGGRAL	15
6D-6	GANTNTGKL	27	14-1	GGYNQGKL	23
9-2	SMGLQQQQT	7	16	RRNSGTYQ	13
16	RETTGSGGKL	44	16	REANSGTYQ	13
3-3	SPSSNMGYKL	9	12-3	RKALAGQYF	49
7-6	RGSGGSNAKL	42	3-3	RSGGSNAKL	42
16	**RVSGGSNAKL**	**42**	7-3	SSRTGGYKV	12
16	REGRTQVVGQL	5	15-1	WELGGSWQL	22
16	REGKGGGSNYKL	53	13-3	ELGTGSNRL	28
			6D-6	GPSSGSWQL	22
			16	REGQGNYQL	33
			16	RDRNSNNRI	31
			4D-3	RRGGSNAKL	42
			7-4	SIRNSNNRI	31
			14-1	RTTGANTGKL	52
			16	**RVSGGSNAKL**	**42**
			16	RASGGSNAKL	42
			16	RGSGGSNAKL	42
			16	RSSGGSNAKL	42
			16	RESGGSNAKL	42
			16	REGTNSAGNKL	17
			16	REGHGSSGNNL	32
			16	REARDYANKM	47
			6-6	GVPHDSGYNKL	11
			16	RGNYGSSGNKL	32
			7-1	ITSMNYNQGKL	23
			7-3	ITSMNYNQGKL	23
			7-6	ITSMNYNQGKL	23

Unlike the TCR β chain repertoire, the TCR α chain repertoires for the NP_{366}/D^b ligand are characterized by their "private" nature. A total of 81 distinct CDR3α clonotypes were detected, 31 after primary infection and 50 after secondary infection, respectively. Note that there was no reduction of the clonality of the TCR α chain repertoires during the transition from primary to secondary immune response. Rather, the complexity appears to have increased considerably. The diverse nature of the TCR α chain repertoires is also clearly reflected by the highly variable length of these distinct CDR3α clonotypes (4–12 amino acid residues but with no five residue CDR3α clonotypes detected). Moreover, the amino acid compositions of the CDR3α loops are extremely diverse. No obvious consensus emerges, except for the CDR3α clonotypes of eight and ten residues (see below).

"Public" and other conserved CDR3α clonotypes with distinct molecular features are identified upon repeated viral exposure

Despite an overall diverse nature, detailed analysis of the TCR α chain repertoires in individual animals has revealed a clear preference for the TRAV16 gene segment in pairing with the TRBV13-1 TCR β chains. As shown in Figure 1, 37.6% of TCR α chains used TRAV16 after primary infection. The percentage of this Vα gene segment increased to 42.6% after a second exposure to virus. Moreover, the TRAV16 gene segment is preferentially combined with either TRAJ42 (20.1% and 28.1% after primary and secondary infection, respectively) or TRAJ13 (7.5% and 14.9% after primary and secondary infection, respectively). Such preferential Vα-Jα combinations were not observed among the non-TRAV16 TCR α chains.

Notes to Table 1:
$CD8^+$ $NP_{366–374}/D^b$ $tetramer^+$ $TRBV13\text{-}1^+$ cells were sorted from the spleens of individual mice after primary or secondary infection with the influenza A virus (three animals per group). The nucleotide sequences of the various elements of the rearranged TCR α chains, including the Vα, Jα gene segment and the hypervariable CDR3α junction regions, were determined by 5′-RACE PCR in combination with a high-throughput DNA sequencing approach as described in detail in Materials and Methods. Shown are the deduced amino acid residues of each CDR3α clonotype with the corresponding V α and J α gene segment usage detected from three mice of each group. Detailed results including frequency of each CDR3 α clonotype from individual mice examined are available in Supplementary Data Table 3. The CDR3α sequences printed in bold face represent the "public" TCR α chain shared by all six individual mice tested in this study. The CDR3α sequences underlined were selected to pair with the "public" TRBV13-1-TRBD1-TRBJ2-2 TCR β chain for molecular modeling and/or TCR gene assembly for transfection studies. See Figure 5(d) and Supplementary Data Table S4 for the amino acid sequences of the three CDR loops of this TCR β chain. The nomenclature for the TCR αβ heterodimers built for this purpose is: A3-4, TRAV16-TRAJ42/TRBV13-1-TRBD1-TRBJ2-2; A1-5, TRAV16-TRAJ31/TRBV13-1-TRBD1-TRBJ2-2; R7-2, TRAV7-3-TRAJ23/TRBV13-1-TRBD1-TRBJ2-2; and R8-5, TRAV7-3-TRAJ31/TRBV13-1-TRBD1-TRBJ2-2.
See Supplementary Data Table S1 for details of the nomenclature.

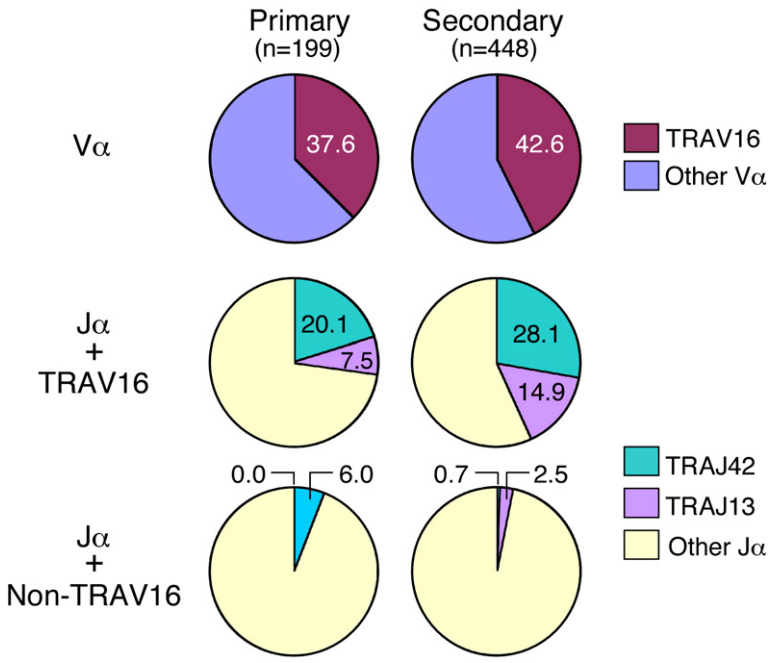

Figure 1. Conservation of TRAV16, TRAJ42 and TRAJ13 segments among Vα domains associated with the highly restricted TRBV13-1-TRBD1-TRBJ2-2 TCR β chain. Vα and Jα gene segment usage of the TCR α chains specific for the NP_{366}/D^b ligand of the influenza A virus were determined as described in Table 1. The analysis was performed on the basis of the data provided in Supplementary Data Table S3. The numbers in each graph represent the calculated percentages of Vα and Jα gene segment usage for data pooled from three individual animals after primary or secondary infection with the influenza A virus. The number of total DNA sequences utilized is given.

Notably, the two conserved CDR3α loops are either ten residues (TRAV16-TRAJ42) or eight residues long (TRAV16-TRAJ13) in length (Table 1). Consensus sequence analysis reveals that, whereas the TRAV16 gene segment-encoded residue (Arg107) was highly conserved even after a primary infection, there is a strong selection of the TRAJ42 gene segment-encoded residues within the ten residue CDR3α region after a second exposure to the virus (Figure 2(a) upper panel), indicating the potentially important role of these residues in the recognition of the NP_{366}/D^b ligand. However, the TRAV16-TRAJ42 junction region-encoded amino acid residues showed considerable variation at position 108 of the loop, with a total of five different amino acid residues recorded, including Val, Ala, Gly, Glu and Ser. Nonetheless, the frequencies of these conserved ten residue CDR3α clonotypes with the RxS recognition motif increased dramatically after a second exposure to influenza A virus (from 50.1% to 89.6%) (Figure 2(b), upper panel). Similar results were obtained with the eight residue CDR3α loops (Figure 2(a), middle panel). Strong selection of almost all amino acid residues within the loops was observed after a second infection, except for the TRAV16-TRAJ13 junction region-encoded residue at position 108, where six amino acid substitutions were observed (Gly, Ala, Arg, Pro, Glu and Thr). Thus, the eight residue CDR3α loops with TRAV16-TRAJ13 and RxN recognition motif represent the second relatively conserved CDR3α clonotype within the overall diverse TCR α chain repertoire. Likewise, there was a selective enrichment of these conserved TRAV16-TRAJ13 TCR α chains after a secondary infection (27.3% *versus* 62.7%, Figure 2(b), lower panel). In contrast, the individual amino acid residues from the highly diverse nine residue CDR3α clonotypes did not show any increase of the usage frequencies from primary to secondary infection (Figure 2(a), lower panel). Nor was there an increase in the frequency of the individual clonotypes within this subset of TCR α chains (data not shown).

One perhaps unexpected result from this comprehensive molecular analysis of the TCR α chain repertoire is the selection of a public TCR α chain despite the diverse TCR α chain repertoire in each animal examined. This public TCR α chain belongs to the conserved TRAV16-TRAJ42 α chain with a ten residue CDR3α loop, and a largely conserved valine residue at position 108, even though this residue is encoded by the N junction region of the TRAV16-TRAJ42 TCR (Table 1; Figure 2(a), upper panel). Most importantly, this public TCR α chain represents one of the most prominent CDR3α clonotypes among the TCR α chains after either primary or secondary infection (14.0% and 13.6%, respectively; Figure 3). The usage of this public TCR α chain within the ten residue CDR3α clonotypes is increased only slightly, from 50.9% to 57.5%, after a second exposure to the same NP_{366}/D^b ligand (Figure 3).

Predicted impact of different TCR α chains on the biophysical nature of the paired public TRB β chain

In order to characterize features of the molecular determinants of the various Vα domains selected, molecular dynamics simulations were performed on Vα-Vβ domain modules of four TCR αβ heterodimers (A3-4, A1-5, R7-2 and R8-5 TCRs; see Supplementary Data Table S1 for the nomenclature of the TCRs), each incorporating the same public TRB β chain but a different TCRα chain. As a result, four TCRs were created, which differ from each other in the following three key aspects of their Vα molecular

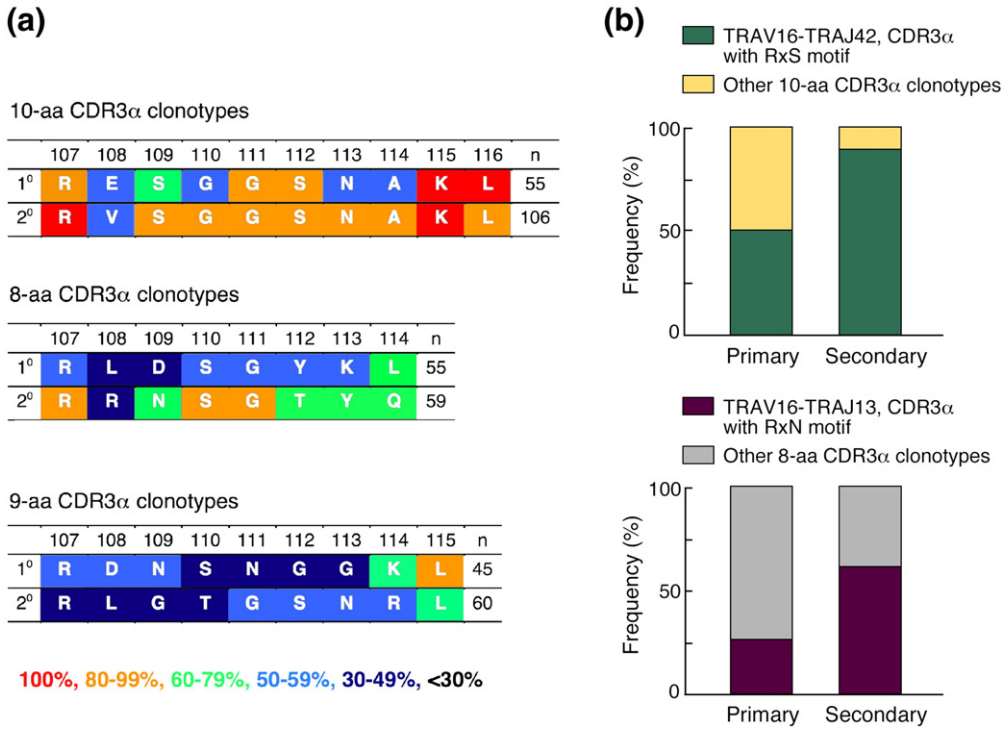

Figure 2. Selection of public and other conserved CDR3α clonotypes with distinct molecular features from the diverse TCR α repertoire. The analysis, utilizing the data provided in Supplementary Data Table S3, represents the results combined from three individual animals after primary (1°) or secondary (2°) infection with the influenza A virus. (a) Consensus amino acid sequences of the CDR3α loops of indicated lengths were analyzed and generated by aligning amino acid sequences from all of the CDR3α clonotypes detected in each group using MegAlign software (DNAStar). The color code for each residue represents the frequency (percentage) of that residue within the corresponding CDR3α clonotype group. The color code key is shown at the bottom. Arg107, the residue at 108 and residues starting from position 109 are encoded by the Vα germline, α N-region and Jα gene segment, respectively. (b) Selective enrichment of the conserved CDR3α clonotypes with RxS or RxN recognition motif during transition from primary to secondary infection with influenza A virus. The x represents V, A, E, S, or G residues for the ten amino acid residue CDR3α clonotype with the RxS motif and G, A, P, E, R, or T residues for the 8-amino acid CDR3α clonotypes with the RxN motif.

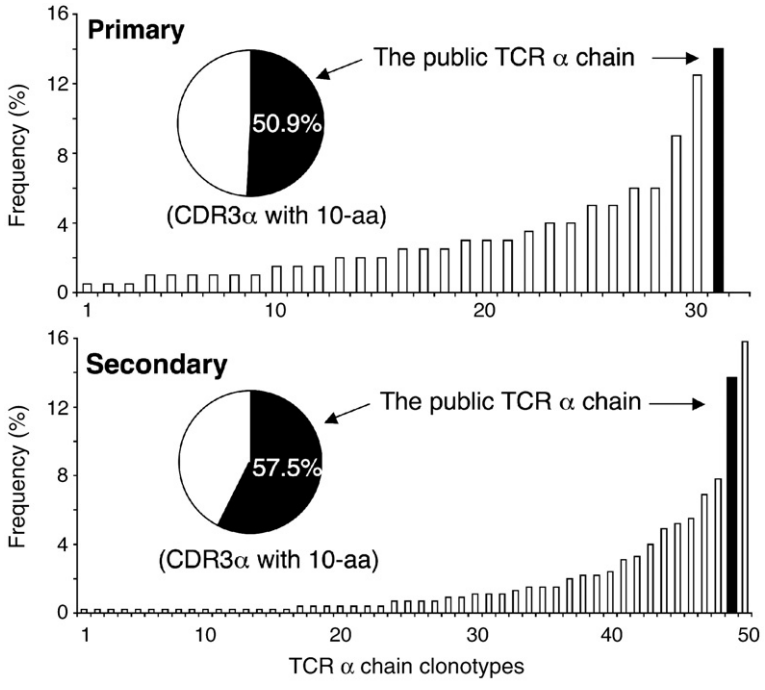

Figure 3. Prominent usage of the public TCR Vα domain within primary and secondary Vα repertoires. Each TCR α clonotype represents a distinct amino acid sequence of a TCR α chain identified from three individual animals after primary (upper panel) or secondary (lower panel) infection. The inset in each Figure shows the percentage of the public TCR α chains among the clonotypes whose CDR3α hypervariable loop are ten amino acid residues in length.

features: (1) Vα gene segment-encoded CDR1α and CDR2α loops (whereas the private A1-5 TCR shares the same TCRα gene segment with the common A3-4 TCR (TRAV16), both R7-2 and R8-5 TCR use a TCRα gene segment (TRAV7-3) that is different from the common A3-4 TCR); (2) the length of the CDR3α loop [A3-4 and R7-2 TCR possess a considerably longer CDR3α loop (10 *versus* 11 amino acid residues, respectively) than A1-5 and R8-5 TCR (six *versus* four amino acid residues, respectively)]; and (3) the amino acid compositions of the CDR3α loops (no consensus can be observed among the four TCRα chains selected). In this way, we could directly compare the common Vβ domain in the context of the independently varied Vα and Jα pairs comprising the distinct Vα domains.

Figure 4 shows backbone representations of the models generated during the molecular dynamics simulation of each Vα-Vβ domain module. The CDR loops were allowed to move freely during the simulation, while the framework was held constant. Figure 4(a) offers a side-view of the A3-4 TCR Vα-Vβ domain module, while Figure 4(b)–(e) show all four TCR modules from the point of view of the pMHC ligand, illustrating the conformations sampled by the CDR loops during the simulations. It is apparent that each TCR displays distinct behavior for its unique α subunit and for the shared β subunit. The size and character of the Vα CDR loops have a direct impact on the conformation and dynamic behavior of the Vβ CDR regions, as is shown in greater detail below.

In order to assess more quantitatively the behavior of each TCR, the root-mean-square deviation (RMSD) was calculated for each residue within the CDR loops as well as for each individual CDR loop over the course of the simulation (Supplementary Data Table S4), using the structure at 500 ps as a reference. Figure 5 shows the calculated RMSD for the public A3-4 CDR loops of (a) the Vα domain and (b) the Vβ domain over the course of the molecular dynamics simulation. In this TCR, the CDRs of Vα exhibit a greater degree of mobility than those of Vβ, as indicated by the frequent variation of RMSD as well as the generally greater magnitude of variation. There seem to be two distinct states for the A3-4 Vβ CDRs during the course of the simulation (Figure 5(b)) as evidenced by the disparity in RMSD for CDR1 and CDR2 from the first 100ps *versus* the final 3500ps.

In comparison, Figure 5(c) shows the RMSD plot of the A1-5 Vβ CDR loops. In particular, CDR2β for this TCR shows a large degree of motion, apparently transitioning between two distinct conformational states more than once. Examining the molecular models of this simulation shows that the βTyr57 residue within its CDR2 loop is largely responsible for this motion *via* a transient interaction with A1-5 CDR3α, particularly the αThr110 and αAsn109 residues therein. This βTyr57 apparently switches between two distinct conformations, as the RMSD plot suggests. Tyr31 within the CDR1β interacts also with this βTyr57 and with Thr110 from CDR3α, but remains relatively stationary throughout the simulation. Comparing A1-5 with the public A3-4 TCR, we find Tyr57 of the public TRB13-2 CDR2β interacts less frequently (and less strongly) with the CDR3α residues, yet maintains its contact with the Tyr31 on CDR1β. The TCR β chain of A3-4 does seem to shift between two states early in the simulation (Figure 5(b)), although this shift is governed largely by CDR3β, most notably the central Asn111 residue (Figure 5(d) and (e)). This interaction highlights the general trend within these experiments in which the Vα affects the conformation and mobility of the Vβ. Indeed, Figure 5(d) shows considerably distinct conformational flexibility for the same residues in the common CDR3β sequence among the four different TCRs. For instance, the central Asn111 exhibits a large range of motion, i.e. greater average RMSD, in the A3-4 TCR and thus, this residue seems quite mobile in this TCR. In contrast, when the same β chain is paired with the TRAV73-23 chain of R7-2 TCR, Asn111 has a smaller range of motion. Conversely, the N-terminal half of the loop for the R8-5 TCR is much more mobile than for any of the others, both in range and frequency of motion (Figure 5(d); Supplementary Data Table S4). Since CDR3α in R8-5 is very short, more freedom of motion is allowed for both CDR2β and CDR3β. Figure 5(e) highlights the striking differences in CDR3β conformation between the four TCRs, despite the fact they share the same sequence.

Impact of distinct TCR α chains on the immunological behavior of resultant TCRs paired with the same public TRB13-2 β chain

The molecular dynamics reveal a dramatic effect of the TCR Vα domains on the biophysical behavior of the entire TCR pMHC recognition module. To test directly the functional impact of these differences, we assembled three TCRs (A3-4, A1-5, and *R7-2*), generated stable transfectants in $58\alpha^{-}\beta^{-}$ $CD8\alpha\beta^{+}$ cells, and then assessed the capability of the resulting cell surface-expressed αβTCRs to recognize the NP_{366}/D^{b} ligand and the functional consequences of the TCR-pMHC engagement using NP_{366}/D^{b} tetramer binding assays and IL-2 assays, respectively.

Flow-cytometry show that three independent clones from each TCR transfectant line express similar levels of the TRB13-2 TCR β chain, CD3ε and CD8αβ molecules on the surface of transfectants (Supplementary Data Figure S1). We investigated the ability of these TCRs to specifically recognize the common NP_{366}/D^{b} ligand of the PR8 and x31 influenza A virus. As shown in Figure 6(a), the strongest NP_{366}/D^{b} tetramer binding (MFI: 311.0±45.0) was observed when the public TRB13-2 β chain was paired with the public TRA16-42 α chain in A3-4. However, when the same public β chain was paired with the private TRA16-31 α chain in the A1-5 TCR, the binding of the resulting A1-5 TCR to the same ligand decreased considerably (MFI: 27.0±5.0). Careful NP_{366}/D^{b} tetramer titration reveals an approximately fourfold difference in the

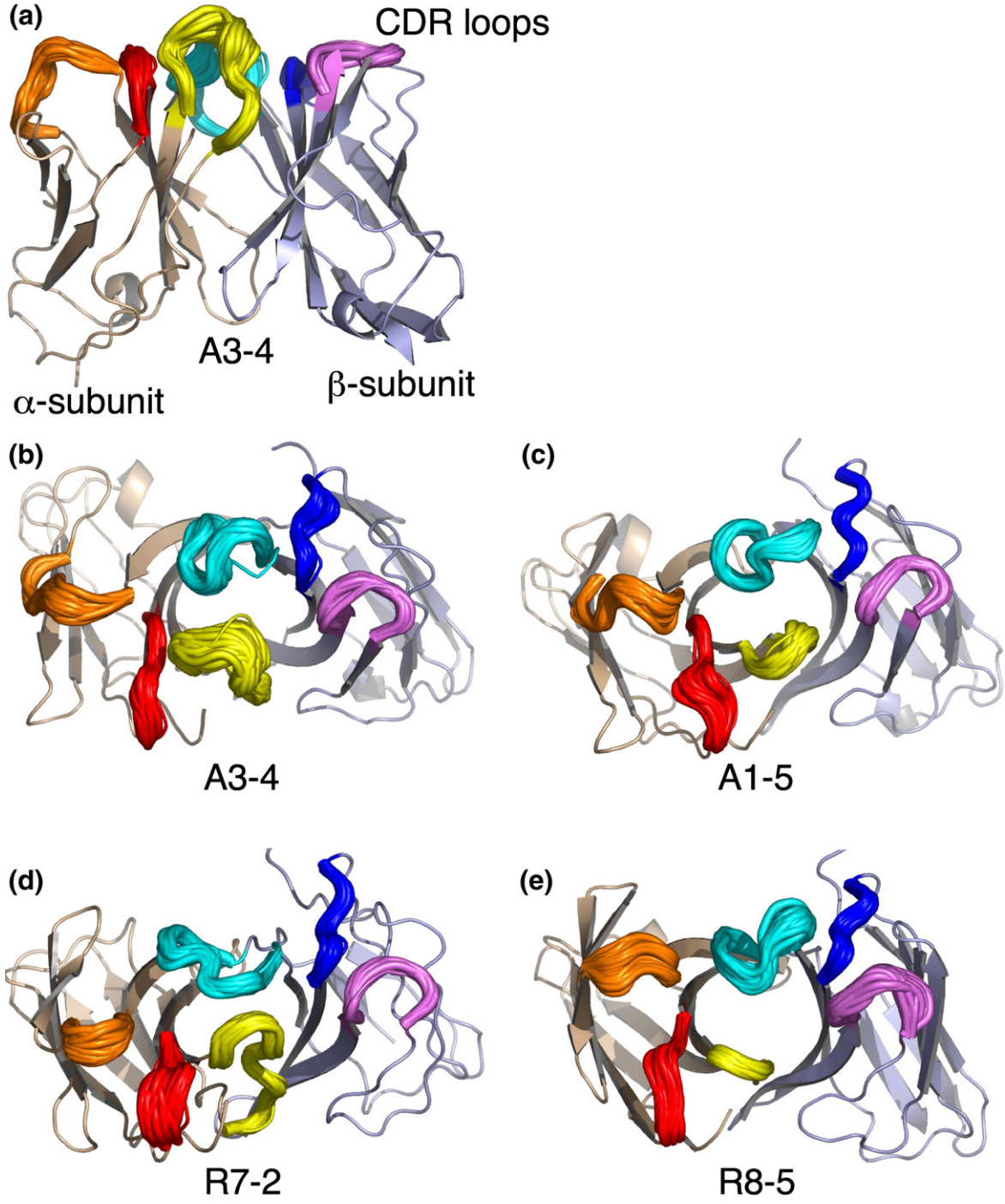

Figure 4. Differential conformations and mobility of the public TRBV13-1-TRBD1-TRAB2-2 Vβ domain when paired with distinct TCR Vα domains. (a) A ribbon diagram of structural models (900 structures over 4.5 ns). The Vα domain is shown in brown for the framework and red, orange and yellow for CDR1, CDR2, and CDR3, respectively. The Vβ domain is shown in grey for the framework and blue, pink, and cyan for CDR1, CDR2, and CDR3. (b)–(e) Ribbon diagrams of all four TCRs are shown from the point of view of the pMHC ligand (90° rotation about the *x*-axis as shown in (a). Color codes are the same as in (a). Nomenclature of TCRs is as defined in Supplementary Data Table S1.

avidity to the pMHC ligand between the A3-4 and the A1-5 TCR. The highest dilution of the NP_{366}/D^b tetramer to achieve a positive binding to A3-4 and A1-5 TCR was the 1:96 and 1:24, respectively (data not shown). Furthermore, when the same public β chain was paired with the private TRA73-23 α chain in R7-2, no detectable tetramer binding was observed (MFI: 4.2±3.2).

The functional consequence of this differential pMHC ligand binding avidity on the three TCR transfectants was examined by measuring their IL-2 production after antigenic stimulation *in vitro*. As

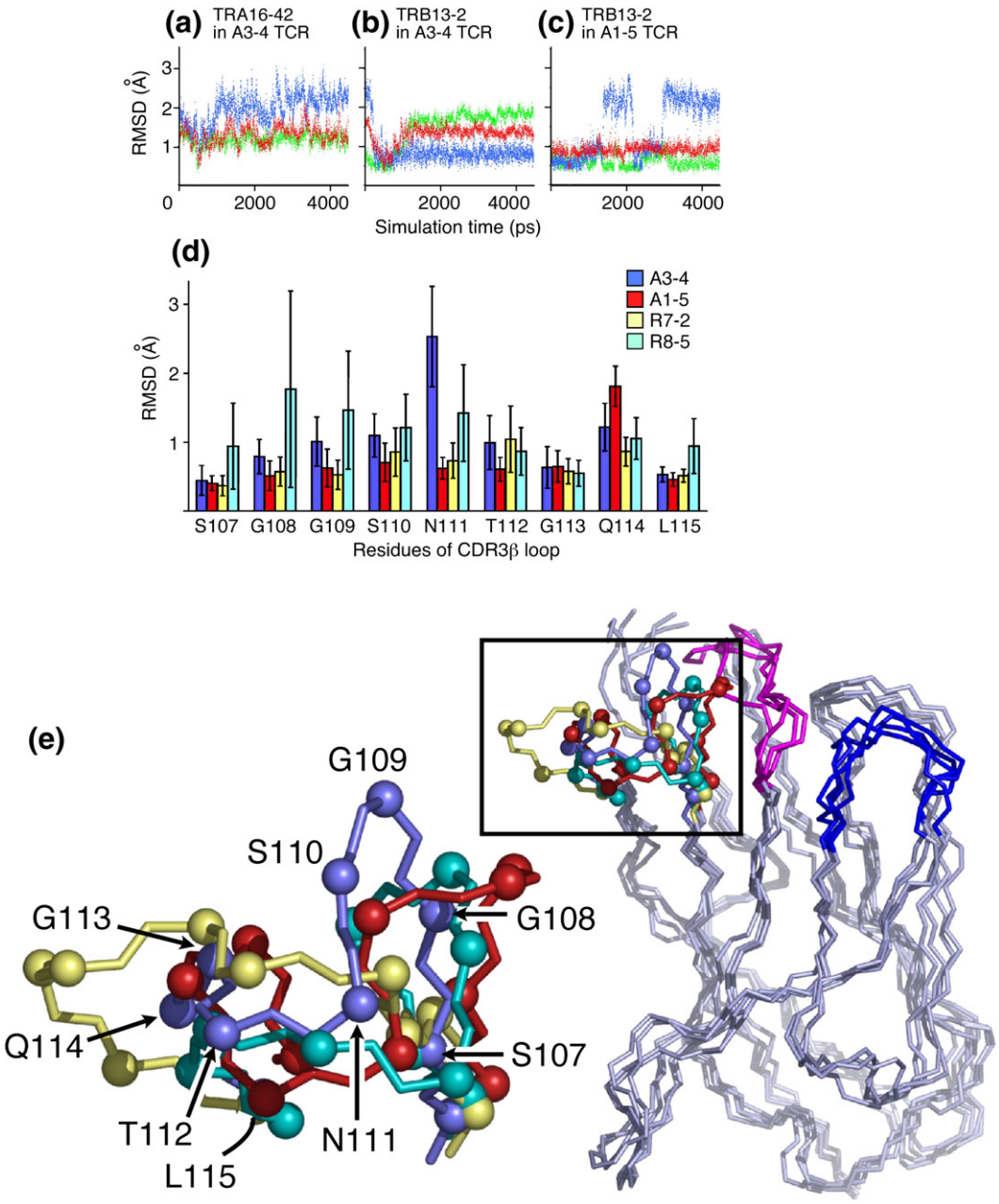

Figure 5. Molecular dynamics of V modules of public and private TCRs specific for NP_{366}/D^b. (a)–(c). RMSD plots, calculated using the 500 ps structure as the reference, for CDR1 (green), CDR2 (blue) and CDR3 (red) of (a) 16–42 α in A3-4 TCR, (b) TRB13-2 β in A3-4 TCR and (c) TRB13-2 β in A1-5 TCR. (d) Average RMSD over 4.5 ns for residues within the CDR3 of the Vβ domains of A3-4 (blue), A1-5 (red), R7-2 (yellow), and R8-5 (cyan) TCRs. Error bars indicate the standard deviation of RMSD over 4.5 ns. (e) Backbone heavy-atom overlay of the final Vβ structure in the molecular dynamics simulation for each TCR. CDR1 (pink), CDR2 (blue), and CDR3 (colored for each TCR as in (d)) are highlighted. The CDR3 region is expanded to highlight the differences in conformation. Balls denote the location of each C^α atom. Residue numbers are indicated for TCR A3-4.

shown in Figure 6(b), upon stimulation with phorbol 12-myristate 13-acetate (PMA)/ionomycin, high-levels of IL-2 (135–250 pg/ml) were detected from the supernatants of all three TCR transfectants, whereas none constitutively produced IL-2 in the absence of stimulus (no peptide control). More importantly, and consistent with the tetramer data described above, productive engagement of the public A3-4 TCR transfectant with the cognate NP_{366}/D^b ligand led to considerable IL-2 production. In contrast, IL-2 production was not detected in the supernatants from either of the two private TCR transfectants (A1-5 and R7-2), although a reproducible but very low level of NP_{366}/D^b tetramer binding was detected in the former case. No IL-2 was detected when the three TCR transfectants were stimulated with an irrelevant PA_{224} peptide bound to the same H-$2D^b$ molecule. Together, these results

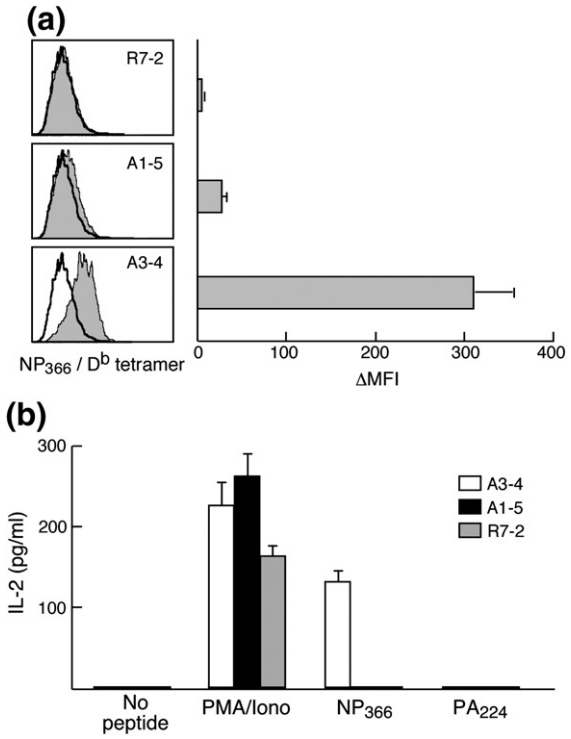

Figure 6. Ligand binding and IL-2 production of T cell transfectants expressing the public TRBV13-1-TRBD1-TRAB2-2 β chain paired with different TCR α chains. (a) NP_{366}/D^b ligand binding by the TCR transfectants. The TCR transfectants were stained at 4 °C for 30 min with the $NP_{366–374}/D^b$ tetramer followed by flow-cytometry. One representative result is shown in the left-hand panel. Solid line: $58\alpha^-\beta^-CD8\alpha\beta^+$ recipient cells. The shaded curve indicates the designated TCR transfectants. The results in the right-hand panel represent the combined data from three separate experiments using three independent clones of each TCR transfectant line described and expressed as the mean and standard deviations of the geometric mean fluorescence intensity of the TCR transfectants minus that of the $58\alpha^-\beta^-CD8\alpha\beta^+$ recipient cells (ΔMFI). (b) IL-2 production by the TCR transfectants upon pMHC stimulation. The TCR transfectants were incubated with mitomycin-treated EL-4 as the APC in the presence of various stimuli as indicated. The IL-2 levels in the supernatants were measured 36 h after stimulation by a cytometric bead array as described in Materials and Methods. One representative experiment is shown from three independent experiments with the same results. For antigen stimulation, peptide concentrations of 10^{-5} to 10^{-10} M were tested but only the maximal results at 10^{-5} M are depicted.

establish that TCR α chains, when paired with the same public TRB13-2 β chain, profoundly impact the ability of the resulting TCRs to interact productively with the NP_{366}/D^b ligand of influenza A virus.

Discussion

Ex vivo molecular tracking of antigen-selected immune αβTCR repertoires has focused on the TCR β chains due to limited tools addressing the diverse nature of TCR α chains.[6] Thus, little is known about the role or diversity of the associated TCR α chains in immune recognition at the αβ TCR population level. Here, we show that 5′-RACE PCR in conjunction with high-throughput DNA sequencing represents a robust approach to characterization of antigen-selected TCR α chain repertoires directly *ex vivo*. Together with computational TCR modeling, molecular dynamics analyses and TCR transfection studies, our results reveal a profound impact of the TCR α chain repertoire on the clonal diversity, structure and function of the resultant αβTCR repertoire selected in response to the D^b-restricted, immunodominant, protective NP_{366} epitope of the influenza A virus such as strains PR8 and x31.

Unexpectedly, a rather diverse TCR α chain repertoire (31 *versus* 50 CDR3α clonotypes after primary and secondary infection, respectively) was found to pair with the highly biased TRBV13-1-derived β chain repertoire (nine *versus* four CDR3β clonotypes after primary and secondary infection, respectively) in order to recognize the NP_{366}/D^b ligand (Table 1).[7] Overall, these TCR α chains are characterized by different Vα and Jα gene segment usage, with a highly variable CDR3 length and amino acid composition. Moreover, no reduction in the clonal TCR heterogeneity was observed after repeated exposure to the influenza A virus. This observation unveils a previously unrecognized versatile aspect of TCR repertoire diversification. That is, the diversity of an antigen-selected TCR repertoire may manifest itself as a highly biased TCR β chain repertoire in conjunction with a diverse TCR α chain repertoire. It is very likely that previous *ex vivo* studies, based solely on the measurement of the antigen-specific TCR β chains, may have considerably underestimated the clonal complexity of the complete αβTCR repertoires. Assuming near-random pairing between the TCR α and β chains identified,[3] an estimated 279 *versus* 200 distinct αβTCRs may be selected in response to stimulation with the NP_{366}/D^b ligand after primary and secondary infection with the influenza A virus, respectively. This considerably expands the breadth of the resultant αβTCR repertoire for the ligand, which has been described as "highly restricted" on the basis of the *ex vivo* TCR β chain repertoire analyses.[7,9] A clear relationship between the TCR repertoire diversity and the antiviral efficacy of specific $CD8^+$ T cells remains to be established. A recent elegant study suggests that a diverse rather than limited TCR β chain repertoire specific for the immunodominant $gB_{495–502}/K^b$ CTL epitope of herpes simplex virus is linked closely to the host's ability to efficiently clear the viral infection.[15] A diverse TCR repertoire is perhaps of key importance in controlling the generation of viral CTL escape variants, as suggested by several independent studies.[16,17] In this regard, pairing of a diverse TCR α chain repertoire with a biased TCR β chain repertoire, as reported here, may represent a novel molecular mechanism to maintain an overall diverse

TCR repertoire to control the escape of the highly heterogeneous influenza A virus from immune surveillance mediated by the virus-specific CTL population, a phenomenon that has been observed to occur after infection of human populations with influenza A virus.[18]

Definition of public and private TCRs has been inconsistent and contradictory in the literature. Cibotti and colleagues first used the terms public and private to describe their finding that murine T cell responses to an immunodominant epitope of hen egg lysozyme involved a TCR β chain component that was shared by all of the individual animals examined (public), and a private TCR β chain repertoire unique to each individual animal (private).[19] Note that the public and private TCRs were defined on the basis of analysis of the TCR β chain repertoire by spectratyping, a technique that characterizes length distribution patterns but not the sequence compositions of CDR3 loops. It has become increasingly clear that different TCR β chains (possibly α chains as well) may share identical V and J gene segment usage and manifest identical lengths of CDR3 loops, but yet have distinct amino acid compositions. Whereas identical TCR β chains that are shared by all of the individuals have been referred to as public TCRs in most reports so far, TCR β chains that are shared by a majority of the individuals examined are considered public TCRs as well in some recent work. Our observation that apart from the public TCR β chains, a public TCR α chain is selected to recognize the NP_{366}/D^b ligand suggests that the pairing possibilities of a public TCR β chain with a TCR α chain, or *vice versa*, may vary considerably. Such pairing may affect the structural nature of the resulting TCRs significantly, and consequently the optimal recognition of the cognate pMHC ligands. This assumption is now supported by our observation that when the same public β chain is paired with different TCR α chains, the resulting TCRs are distinct structurally and immunologically (see below). In light of these observations, our definition of a public TCR, such as the A3-4 TCR studied here, refers to a TCR that consists of a public TCR β chain and a public TCR α chain whose amino acid sequences are shared by all of the individuals with an identical MHC haplotype. TCRs with only one of the two chains being public, such as the A1-5, R7-2 and R8-5 TCR, we consider as private.

At present, the molecular mechanisms for antigen-driven selection of public *versus* private TCRs are poorly understood. Clearly, the thymic selection process during T cell development may play an important part by shaping the nature of naïve TCR repertoires, as indicated in several studies.[20,21] Recent crystallographic studies of TCR-pMHC complexes suggest that the intrinsic structural features of the public TCRs and/or immunodominant pMHC ligands may represent another important factor that controls selection of public *versus* private TCRs after antigen exposure. It has been observed, for example, that the public LC13 TCR underwent extensive conformational changes in the CDR loops upon recognizing the EBNA3A-HLA-B8 ligand derived from Epstein-Barr virus, including both CDR3 loops, and the germline-encoded CDR1α and CDR2α loops, resulting in induced "fit" of the LC13 TCR with the pMHC ligand.[22] Recent structural studies of the influenza A virus-derived immunodominant peptides complexed with mouse $H\text{-}2D^b$ molecules show that surface-exposed structural features of the viral pMHC ligands correlate with their corresponding TCR β chain repertoires selected after *in vivo* infection with the virus.[23] Collectively, these studies suggest that a structural basis may exist for selection of public *versus* private TCRs.

In the present study, a robust model system was created that offers the potential to address the fundamental selective pressure on the public *versus* private TCRs at the population level. Assuming random αβ pairing, a panel of four TCRs was assembled by pairing the public TRB13-2 β chain with either the public TRAV16-42 α chain or one or another private TCR α chain identified in the present study. While the resultant TCRs may or may not all represent *bona fide* TCRs for the NP_{366}/D^b ligand *per se*, they provided us with a unique opportunity to examine the impact of the independently varied TCR α chains on the biophysical nature of the resultant αβTCRs. Unexpectedly, each of the four TCRs modeled display distinct molecular dynamics behavior, both with regard to the mobility of the CDR loops as a whole and with regard to the individual residues within the loops (Figure 4; and Supplementary Data Table S4). Admittedly, without actual NMR or crystal structures, we cannot verify the atomic details of the modeled interactions between the TCR Vβ and associated Vα domains. However, it is likely that subtle structural differences among Vα domains may occur due to distinct physiochemical properties of the amino acid residues among public and private Vα domains, which in turn will considerably affect the biophysical behavior and structural nature of the TCR α chains themselves and/or the paired TCR β chain. Such impact is indeed suggested by our molecular dynamics data. The reduced binding avidity of the private A1-5 TCR, for example, might be the consequence of the transient interaction between the Tyr57 residue within the CDR2β loop and the Asn109 and Thr110 residues of the CDR3α loop (Figure 5(c)), restricting a CDR3α conformational change required for optimal interaction with the NP_{366}/D^b ligand. In contrast, those molecular interactions are not observed when the public A3-4 TCR is analyzed under the same simulation conditions, perhaps reflecting a more optimal biophysical and structural complementarity of the public Vα and Vβ domains. This difference might afford the public TCR a more optimal recognition of the NP_{366}/D^b ligand after infection with influenza A virus.

The public A3-4 TCR consistently showed the best NP_{366}/D^b ligand binding avidity (Figure 6(a)). In

contrast, only marginal binding was observed between the private A1-5 TCR and the pMHC ligand. The binding of the private R7-2 TCR to the NP_{366}/D^b ligand was not detected under the same experimental conditions. The different immunological behavior of the three TCRs did not result from expression levels of the TCRs and CD8αβ heterodimers on the surface of these TCR transfectants, as these were comparable among different clones of the three TCR transfectant lines studied (Supplementary Data Figure S1). Most likely, that difference reflects the structural "fitness" of the public *versus* the private TCRs generated to the $NP_{366–374}/D^b$ ligand studied herein, as clearly suggested by our molecular dynamics data. The public A3-4 TCR, composed of both a public TCR β chain and a public α chain, may be best suited for NP_{366}/D^b ligation. A1-5 TCR, with the same germline-encoded CDR1α and CDR2α loop as those of the public TRAV16-42 α chain of the A3-4 TCR yet a shorter CDR3α loop (six amino acid residues) and distinct amino acid residues, bound to the pMHC ligand with an avidity below the threshold required for T cell activation. The R7-2 TCR, whose CDR2α loop amino acid compositions differed from those of the public TCR α chain, failed to recognize the NP_{366}/D^b ligand. While those two private TCRs as assembled *in vitro* here may not mirror the *bona fide* pairing of TCR α and β chains specific for the NP_{366}/D^b ligand *in vivo*, our data establish the dramatic functional impact of the TCR α chains on the binding avidity of the resulting TCRs to the $NP_{366–374}/D^b$ ligand (Figure 6(b)). Because multiple TCR α chains are associated with the common β chain, analogous consequences of combinatorial pairing may be operative among different αβ TCR heterodimers. Future studies investigating the proliferative and cytolytic potential of CTL clones bearing public *versus* private TCRs are needed to assess other potential links between structure and function of the public *versus* the private TCRs studied here.

The critical role of TCR α chains in T cell development and in shaping of preimmune TCR repertoires have been documented.[24,25] Here, for the first time, we show a profound impact of the TCR α chain repertoire on the clonal diversity, biophysical nature and immune recognition ability of the resulting TCRs selected to the immunodominant, protective NP_{366}/D^b ligand of influenza A virus. These results provide new insights into the fundamental factors that control antigen-driven selection of public *versus* private TCRs, and may have important implications in the development of cellular immunity-based vaccines and immune monitoring of responses against certain viral infections. Induction of an overall diverse TCR repertoire that retains a considerable proportion of the high-avidity public TCRs may be highly beneficial, allowing the host to clear certain viral infections such as influenza efficiently while maintaining sufficient diversity to control viral CTL escape mutants.

Materials and Methods

Mice and influenza A virus

Female C57BL/6 mice (six to eight weeks old) were purchased from Taconic (Albany, NY) and housed under mouse pathogen-free conditions at the animal core facility of the Dana-Farber Cancer Institute (DFCI). The strains of influenza A virus used in this study, and primary and secondary infection of mice with these strains (A/PR8/8/34 (PR8, HIN1) and A/HK/x31 (x31, H3N2), respectively) were as described.[26] Viral inoculation of the animals, the subsequent housing and tissue sampling were conducted under BL2 conditions at DFCI according to a protocol reviewed and approved by the Animal Care and Use Committee.

Flow cytometry

APC or PE-conjugated NP_{366}/D^b tetramer was purchased from Beckman Coulter, Inc. (San Diego, CA). FITC or PE-conjugated anti-mouse TRBV13-1, TRBV2 and CD8α were purchased from BD Pharmingen. Immunostaining and sorting of the $CD8^+$ NP_{366}/D^b $tetramer^+$ $TRBV13\text{-}1^+$ cells from the spleen of the virus-infected mice were as described.[7] The purity of the sorted cells was typically >96% in this study.

5′-RACE PCR

Total RNA was extracted from 4000–200,000 sorted $CD8^+$ NP_{366}/D^b $tetramer^+$ $TRBV13\text{-}1^+$ cells as described.[7] Our initial analysis of the NP_{366}/D^b-specific Vα repertoire indicates that the TCR Vα repertoire pairing with the highly biased TRBV13-1 TCR β repertoire is itself diverse. Therefore, a 5′-RACE approach was used to amplify the diverse TCR α chain transcripts. Briefly, total RNA was first reverse-transcribed to cDNA using a SMART RACE cDNA amplification kit (BD Clontech) according to the manufacturer's instructions. The 5′-RACE cDNA products were then amplified by a nested PCR. The primers used for the nested PCR were as follows: 5′ universal primer mix A (BD Clontech) in combination with the first gene-specific 3′ Cα primer (GGCAGGTGAAGCTTGTCTGGTTGCTCCA) was employed for the first round of amplifications. A nested universal primer (BD Clontech) in combination with the second gene-specific 3′ Cα primer (GTCAAAGTCGGTGAACAGGC) were used for the second round amplification using 1 μl of 1:50–1:100 (v/v) diluted first-round PCR products as templates. The PCR procedure included 2 min at 95 °C, followed by 30 cycles of 94 °C for 30 s, 68 °C for 30 s, and 72 °C for 2 min. A final extension step was performed at 72 °C for 10 min. Gel electrophoresis analysis of the 5′-RACE PCR products generated from a naïve $CD8^+$ $CD44^{low}$ $TRBV13\text{-}1^+$ cell population revealed that a complete collection of the heterogeneous TCR α gene transcripts was amplified under the experimental conditions described above. These results demonstrate both the efficiency and the reliability of the approach for the analysis of a diverse TCR Vα repertoire (data not shown).

Cloning of 5′-RACE PCR products for high-throughput DNA sequencing

5′-RACE PCR products were extracted from 2% (w/v) agarose gels using a QIAquick gel extraction kit (Qiagen).

Cloning of the purified 5′-RACE PCR products into the pCRII-TOPO vector, bacterial growth and preparation of plasmid DNA were as described.[7] From 96 to 240 single, white colonies were picked from each cloning reaction and grown in 96-well plasmid preparation plates (Montage Plasmid Kit, Millipore). High-throughput DNA sequencing was performed at Dana-Farber/Harvard Cancer Center, Cambridge, MA, using forward and reverse M13 primers. The success rate of this approach was typically 60–85% in this study.

DNA sequence processing and TCR gene assignment

An in-house computer-based program was used to process the large number of TCR Vα sequences generated in this study. This program can assign the Vα and Jα usage of individual mouse TCR Vα chains according to the TCR nomenclature of the International ImMunoGeneTics (IMGT) Database System,[27] and outputs the nucleotide sequences of the corresponding CDR3α regions, which are further analyzed by DNAstar software (DNASTAR Inc.).

TCR modeling and molecular dynamics analysis

Four TCR α chains were selected from the α chain repertoire analysis to be paired with the public TCR β chain identified earlier.[7] The deduced αβ TCR sequences were used for molecular modeling and the subsequent molecular dynamics analysis. The nomenclatures and numbering of the TCRs built as well as the amino acid sequences of the CDR loops are indicated in Table 1 and described in detail in Supplementary Data Table S1.

Homology models of the selected four unliganded TCRs were built with MODELER,[28] using the previously solved crystal structure of murine TCR 2C as a template.[29] The conformations of the side-chains in the modeled TCR domains were predicted by the SCWRL3 algorithm[30] except for residues located in the CDR3 loops, which were predicted by the hierarchical technique implemented in Prime.[31] All the conformations within 10kcal/mol of the lowest were retained for further analysis. The TCR models were analyzed using PyMol visualization software (http://www.pymol.org).

All atom molecular dynamics simulations were performed on four different TCR α-β heterodimer structures derived from the homology modeling. The protein was solvated in a truncated octahedral box of TIP3P water molecules extending to 12 Å from the surface of the protein.[32] Requisite numbers of counter ions were placed randomly in the simulation box to maintain net neutral charge on the system. All simulations were carried out with the AMBER software suite† using the parm99sb force field.[33] A simulation time-step of 0.2 fs was employed along with the SHAKE algorithm to constrain the heavy atom – hydrogen bond lengths.[34] The particle mesh Ewald method was used to treat long-range electrostatics along with an 8.0 Å cutoff to limit the direct space sum.[35,36] During the equilibration phase of the simulation, the system was heated slowly to 300 K, the simulation temperature, with strong 25 kcal/mol per Å restraints on the protein atom positions. Over the course of 100 ps the ion and water positions were freely equilibrated and the restraints on the protein atom positions were decreased slowly to 0.5 kcal/mol per Å. The production simulation was pursued after raising the restraint on the non-CDR loop regions of the protein to 25 kcal/mol per Å while the CDR loops of interest were free to move. Molecular dynamics simulation for 5 ns was carried out for each of the four TCR structures to analyze the differences in loop conformational dynamics.

† http://www.amber.scripps.edu

TCR gene assembly and expression vectors

The rearranged gene elements encoding the four full-length TCR α chains and the β chain were assembled by PCR approaches (see Supplementary Data, including Table S2). Plasmid vector pSHxs and pBJneo were used for expression of the TCR β and TCR α chains, respectively.[37] To subclone the TCRs into the expression vectors, cDNA fragments encoding the full-length TCRs were excised by double digestion with either XhoI/SacI (for TCR β chain) or XhoI/EcoRI (for TCR α chains), isolated by gel extraction and then ligated into pSHxs and pBJneo expression vector linearized with BglII/SalI or BglII alone, respectively. The expression vectors were transformed into Top 10 competent cells (Invitrogen). Plasmids were prepared from the positive colonies on LB selection plates and sequenced to ensure the insertion of the rearranged, error-free TCR genes.

Transfection of the mouse T cell hybridoma $58\alpha^-\beta^-CD8\alpha\beta^+$ cells

The $58\alpha^-\beta^-CD8\alpha\beta^+$ cells are TCR$^-$ murine T hybridoma cells expressing all CD3 subunits and murine CD8αβ heterodimers.[37] Each sample of 1×10^7 $58\alpha^-\beta^-CD8\alpha\beta^+$ recipient cells was transfected in a Gene Pulse Cuvette (Life Technology) with 10 μg of the public TRB13-2 TCR β chain-encoding the pSHxs vector and 25 μg of TRA16-42, TRA16-31, or TRA73-23 TCR α chain-encoding the pBJneo vector by electroporation at 250 V and 800 mF. At 48 h after transfection, the cells were plated in 24-well plates at 2×10^4 cells/well in the complete RPMI 1640 medium containing 0.1 mg/ml of G418 (GIBCO) and 2 mg/ml of Hygromycin B (Roche). The resistant cell cultures were screened two weeks later by flow-cytometry for surface expression of the murine TCR TRB13-2 chain. Three TRB13-2-positive clones were selected from each TCR transfectant line and further sorted by flow-cytometry to enrich those clones that express high-level TCR on the cell surface.

Determination of IL-2 production by the TCR transfectants

To generate APCs, each 2×10^7 EL-4 cells were treated with 50 μg/ml mitomycin (Novaplus) in 2 ml of complete RPMI1640 medium at 37 °C for 20–25 min followed by extensive washing. Each sample of 2×10^5 TCR transfectants was incubated in triplicate with equal numbers of the mitomycin-treated EL-4 cells in 200 μl of complete RPMI1640 medium in the presence of various stimuli, including PMA/ionomycin, 10^{-5} M influenza A/PR8 virus-derived NP_{366} or $PA_{224–233}$ (PA_{224}) synthetic peptide, or no peptide as a negative control. At 36 h after incubation, 50–75 μl supernatant was harvested from each well and IL-2 production by the TCR transfectants was determined with a mouse Th1/Th2 cytokine Cytometric Bead Array (BD) according to the manufacturer's

instructions. The detection sensitivity of the assay is 20 pg/ml of IL-2.

Acknowledgements

We thank Dr Hsiu-Ching Chang for kindly providing the TCR expression vectors, and the N15α and N15β plasmids; Drs Zhisong Qiao and Yoon-Joong Kang for assistance in TCR gene assembly and TCR transfection studies; Dr Pedro Reche for help in developing the Pargrep.pl computer program for the analyses of the TCR α chain sequences and Ms Maris Handley for assistance with flow cytometry. This study was supported by a pilot project award to W.Z. from a Public Health Service grant U19 AI57330 and AI19807 to ELR and AI37581 to G.W.

Supplementary Data

Supplementary data associated with this article can be found, in the online version, at doi:10.1016/j.jmb.2007.06.057

References

1. Ahmed, R. & Gray, D. (1996). Immunological memory and protective immunity: understanding their relation. *Science*, **272**, 54–60.
2. Zinkernagel, R. M. & Doherty, P. C. (1974). Restriction of *in vitro* T cell-mediated cytotoxicity in lymphocytic choriomeningitis within a syngeneic or semiallogeneic system. *Nature*, **248**, 701–702.
3. Davis, M. M. & Bjorkman, P. J. (1988). T-cell antigen receptor genes and T-cell recognition. *Nature*, **334**, 395–402.
4. Rudolph, M. G., Stanfield, R. L. & Wilson, I. A. (2006). How Tcrs bind Mhcs, peptides, and coreceptors. *Annu. Rev. Immunol.* **24**, 419–466.
5. Wang, J.-H. & Reinherz, E. (2001). Structural basis of T cell recognition of peptides bound to MHC molecules. *Mol. Immunol.* **38**, 1039–1049.
6. Rufer, N. (2005). Molecular tracking of antigen-specific T-cell clones during immune responses. *Curr. Opin. Immunol.* **17**, 417–441.
7. Zhong, W. & Reinherz, E. L. (2004). *In vivo* selection of a TCR V beta repertoire directed against an immunodominant influenza virus CTL epitope. *Int. Immunol.* **16**, 1549–1559.
8. Crowe, S. R., Miller, S. C. & Woodland, D. L. (2006). Identification of protective and non-protective T cell epitopes in influenza. *Vaccine*, **24**, 452–456.
9. Kedzierska, K., Turner, S. J. & Doherty, P. C. (2004). Conserved T cell receptor usage in primary and recall responses to an immunodominant influenza virus nucleoprotein epitope. *Proc. Natl Acad. Sci. USA*, **101**, 4942–4947.
10. Argaet, V. P., Schmidt, C. W., Burrows, S. R., Silins, S. L., Kurilla, M. G., Doolan, D. L. *et al.* (1994). Dominant selection of an invariant T cell antigen receptor in response to persistent infection by Epstein-Barr virus. *J. Expt. Med.* **180**, 2335–2340.
11. Naumov, Y. N., Hogan, K. T., Naumova, E. N., Pagel, J. T. & Gorski, J. (1998). A class I MHC-restricted recall response to a viral peptide is highly polyclonal despite stringent CDR3 selection: implications for establishing memory T cell repertoires in "real-world" conditions. *J. Immunol.* **160**, 2842–2852.
12. Cose, S. C., Kelly, J. M. & Carbone, F. R. (1995). Characterization of diverse primary herpes simplex virus type 1 gB-specific cytotoxic T-cell response showing a preferential V beta bias. *J. Virol.* **69**, 5849–5852.
13. Pantaleo, G., Demarest, J. F., Soudeyns, H., Graziosi, C., Denis, F., Adelsberger, J. W. *et al.* (1994). Major expansion of CD8+ T cells with a predominant V beta usage during the primary immune response to HIV. *Nature*, **370**, 463–467.
14. Pewe, L. & Perlman, S. (1999). Immune response to the immunodominant epitope of mouse hepatitis virus is polyclonal, but functionally monospecific in C57Bl/6 mice. *Virology*, **255**, 106–116.
15. Messaoudi, I., Guevara Patino, J. A., Dyall, R., LeMaoult, J. & Nikolich-Zugich, J. (2002). Direct link between mhc polymorphism, T cell avidity, and diversity in immune defense. *Science*, **298**, 1797–1800.
16. Lewicki, H., Tishon, A., Borrow, P., Evans, C. F., Gairin, J. E., Hahn, K. M. *et al.* (1995). CTL escape viral variants. I. Generation and molecular characterization. *Virology*, **210**, 29–40.
17. Pircher, H., Moskophidis, D., Rohrer, U., Burki, K., Hengartner, H. & Zinkernagel, R. M. (1990). Viral escape by selection of cytotoxic T cell-resistant virus variants *in vivo*. *Nature*, **346**, 629–633.
18. Voeten, J. T., Bestebroer, T. M., Nieuwkoop, N. J., Fouchier, R. A., Osterhaus, A. D. & Rimmelzwaan, G. F. (2000). Antigenic drift in the influenza A virus (H3N2) nucleoprotein and escape from recognition by cytotoxic T lymphocytes. *J. Virol.* **74**, 6800–6807.
19. Cibotti, R., Cabaniols, J. P., Pannetier, C., Delarbre, C., Vergnon, I., Kanellopoulos, J. M. & Kourilsky, P. (1994). Public and private V beta T cell receptor repertoires against hen egg white lysozyme (HEL) in nontransgenic *versus* HEL transgenic mice. *J. Expt. Med.* **180**, 861–872.
20. Correia-Neves, M., Waltzinger, C., Mathis, D. & Benoist, C. (2001). The shaping of the T cell repertoire. *Immunity*, **14**, 21–32.
21. Huseby, E. S., White, J., Crawford, F., Vass, T., Becker, D., Pinilla, C. *et al.* (2005). How the T cell repertoire becomes peptide and MHC specific. *Cell*, **122**, 247–260.
22. Kjer-Nielsen, L., Clements, C. S., Brooks, A. G., Purcell, A. W., McCluskey, J. & Rossjohn, J. (2002). The 1.5 A crystal structure of a highly selected antiviral T cell receptor provides evidence for a structural basis of immunodominance. *Structure (Camb.)*, **10**, 1521–1532.
23. Meijers, R., Lai, C. C., Yang, Y., Liu, J. H., Zhong, W., Wang, J. H. & Reinherz, E. L. (2005). Crystal structures of murine MHC Class I H-2 D(b) and K(b) molecules in complex with CTL epitopes from influenza A virus: implications for TCR repertoire selection and immunodominance. *J. Mol. Biol.* **345**, 1099–1110.
24. Yokosuka, T., Takase, K., Suzuki, M., Nakagawa, Y., Taki, S., Takahashi, H. *et al.* (2002). Predominant role of T cell receptor (TCR)-alpha chain in forming preimmune TCR repertoire revealed by clonal TCR reconstitution system. *J. Expt. Med.* **195**, 991–1001.
25. Ferreira, C., Furmanski, A., Millrain, M., Bartok, I., Guillaume, P., Lees, R. *et al.* (2006). TCR-alpha CDR3 loop audition regulates positive selection. *J. Immunol.* **177**, 2477–2485.

26. Zhong, W., Reche, P. A., Lai, C. C., Reinhold, B. & Reinherz, E. L. (2003). Genome-wide characterization of a viral cytotoxic T lymphocyte epitope repertoire. *J. Biol. Chem.* **278**, 45135–45144.
27. Lefranc, M. P. (2001). IMGT, the international ImMunoGeneTics database. *Nucl. Acids Res.* **29**, 207–209.
28. Sali, A. & Blundell, T. L. (1993). Comparative protein modelling by satisfaction of spatial restraints. *J. Mol. Biol.* **234**, 779–815.
29. Garcia, K. C., Degano, M., Stanfield, R. L., Brunmark, A., Jackson, M. R., Peterson, P. A. *et al.* (1996). An alphabeta T cell receptor structure at 2.5 Å and its orientation in the TCR-MHC complex. *Science*, **274**, 209–219.
30. Canutescu, A. A., Shelenkov, A. A. & Dunbrack, R. L., Jr (2003). A graph-theory algorithm for rapid protein side-chain prediction. *Protein Sci.* **12**, 2001–2014.
31. Jacobson, M. P., Pincus, D. L., Rapp, C. S., Day, T. J., Honig, B., Shaw, D. E. & Friesner, R. A. (2004). A hierarchical approach to all-atom protein loop prediction. *Proteins: Struct. Funct Genet.* **55**, 351–367.
32. Jorgensen, W. L., Chandrasekar, J., Madura, J. & Klein, M. L. (1983). Comparison of simple potential functions for simulating liquid water. *J. Chem. Phys.* **79**, 926–935.
33. Hornak, V., Abel, R., Okur, A., Strockbine, B., Roitberg, A. & Simmerling, C. (2006). Comparison of multiple Amber force fields and development of improved protein backbone parameters. *Proteins: Struct. Funct Genet.* **65**, 712–725.
34. Ryckaert, J.-P., Ciccotti, G. & Berendsen, H. J. (1977). Numerical integration of the cartesian equations of motion of a system with constraints: molecular dynamics of n-alkanes. *J. Comput. Phys.* **23**, 327–341.
35. Darden, T. A., York, D. M. & Pedersen, L. G. (1993). Particle mesh Ewald: an N log (N) method for Ewald sums in large systems. *J. Chem. Phys.* **98**, 10089–10092.
36. Essmann, U., Perera, L., Berkowitz, M. L., Darden, T., Lee, H. & Pedersen, L. G. (1995). A smooth particle mesh Ewald method. *J. Chem. Phys.* **103**, 8577–8593.
37. Chang, H. C., Smolyar, A., Spoerl, R., Witte, T., Yao, Y., Goyarts, E. C. *et al.* (1997). Topology of T cell receptor-peptide/class I MHC interaction defined by charge reversal complementation and functional analysis. *J. Mol. Biol.* **271**, 278–293.

Edited by I. Wilson

(Received 3 April 2007; received in revised form 13 June 2007; accepted 18 June 2007)
Available online 27 June 2007